Astronomy & Astrophysics manuscript no.
(will be inserted by hand later)

Theoretical isochrones in several photometric systems

I. Johnson-Cousins-Glass, HST/WFPC2, HST/NICMOS, Washington, and ESO Imaging Survey filter sets

L. Girardi[1,2], G. Bertelli[3,4], A. Bressan[4], C. Chiosi[1],
M.A.T. Groenewegen[5,6], P. Marigo[1], B. Salasnich[1], A. Weiss[7]

[1] Dipartimento di Astronomia, Università di Padova, Vicolo dell'Osservatorio 2, I-35122 Padova, Italy
[2] Osservatorio Astronomico di Trieste, Via Tiepolo 11, I-34131 Trieste, Italy
[3] Istituto di Astrofisica Spaziale, CNR, Via del Fosso del Cavaliere, I-00133 Roma, Italy
[4] Osservatorio Astronomico di Padova, Vicolo dell'Osservatorio 5, I-35122 Padova, Italy
[5] PACS ICC-team, Instituut voor Sterrenkunde, Celestijnenlaan 200B, B-3001 Heverlee, Belgium
[6] European Southern Observatory, Karl-Schwarzschild-Str. 2, D-85740 Garching bei München, Germany
[7] Max-Planck-Institut für Astrophysik, Karl-Schwarzschild-Str. 1, D-85740 Garching bei München, Germany

Received 05-11-01 / Accepted 19-04-02

Abstract. We provide tables of theoretical isochrones in several photometric systems. To this aim, the following steps are followed: (1) First, we re-write the formalism for converting synthetic stellar spectra into tables of bolometric corrections. The resulting formulas can be applied to any photometric system, provided that the zero-points are specified by means of either ABmag, STmag, VEGAmag, or a standard star system that includes well-known spectrophotometric standards. Interstellar absorption can be considered in a self-consistent way. (2) We assemble an extended and updated library of stellar intrinsic spectra. It is mostly based on "non-overshooting" ATLAS9 models, suitably extended to both low and high effective temperatures. This offers an excellent coverage of the parameter space of $T_{\rm eff}$, $\log g$, and [M/H]. We briefly discuss the main uncertainties and points still deserving more improvement. (3) From the spectral library, we derive tables of bolometric corrections for Johnson-Cousins-Glass, HST/WFPC2, HST/NICMOS, Washington, and ESO Imaging Survey systems (this latter consisting on the WFI, EMMI, and SOFI filter sets). (4) These tables are used to convert several sets of Padova isochrones into the corresponding absolute magnitudes and colours, thus providing a useful database for several astrophysical applications. All data files are made available in electronic form.

Key words. Stars: fundamental parameters – Hertzprung-Russell (HR) and C-M diagrams

1. Introduction

One of the primary aims of stellar evolution theory is that of explaining the photometric data – eg. colour-magnitude diagrams (CMDs), luminosity functions, colour histograms – of resolved stellar populations. To allow whatever comparison between theory and data, the basic output of stellar models – the surface luminosity L and effective temperature $T_{\rm eff}$ – must be first converted into the observable quantities, i.e. magnitudes and colours. This conversion is performed by means of bolometric corrections (BC) and $T_{\rm eff}$-colour relations, and later by considering the proper distance, absorption and reddening of the observed population, and the photometric errors.

Send offprint requests to: Léo Girardi
e-mail: Lgirardi@ts.astro.it

Determining BCs and $T_{\rm eff}$-colour relations is indeed one of the most basic tasks in stellar astrophysics. Empirical determinations (see e.g. the compilations by Schmidt-Kaler 1982, Flower 1996, and Alonso et al. 1999ab) involve a great observational effort, and are obviously the most reliable if compared to purely theoretical determinations. However, since the empirical calibrations are mostly based on nearby stars, only a limited region in the space of stellar parameters ($T_{\rm eff}$, $\log g$, and metallicity [M/H]) can be covered by observations. This contrasts with our present-day capabilities of getting resolved photometry of populations that are certainly very different from the local one, like those in dwarf galaxies and in the Bulge. For instance, present empirical relations do not include young-metal poor populations, or super-metal rich stars, which are likely present in the resolved galaxies of the Local Group.

Another important limitation of empirical relations is that they are usually available just for a small set of filters or photometric systems, like the popular Johnson-Cousins-Glass one. Again, this is in contrast with the rapid diffusion in the use of specific filter sets, for which no empirical relation is yet available, though large databases are already being collected. Just to mention a few relevant examples, new filter sets have been adopted in the Hubble Space Telescope (HST) Wide Field Planetary Camera 2 (WFPC2), in the European Southern Observatory (ESO) Wide Field Imager (WFI), and in the Hipparcos mission. Moreover, brand-new photometric systems have been designed for the Sloan Digital Sky Survey (SDSS), and will be adopted in the future GAIA mission. An impressive amount of data will be provided by these instruments in the coming years, and much of it will soon become of public access. Then, it would be highly desirable to have the capability of converting stellar models to these many new photometric systems, bypassing for a moment the time-consuming procedure of empirical calibration.

With this target in mind, we have undertaken a project aiming at providing theoretical BCs and colour transformations for *any* broad-band photometric system, and many intermediate-band systems as well. Actually, the project starts with the work by Bertelli et al. (1994), who presented a large database of theoretical isochrones and converted them to the Johnson-Cousins-Glass $UBVRIJHK$ system. The transformations were primarily based on Kurucz (1993) synthetic atmosphere models, suitably extended in the intervals of lower and higher effective temperatures. In Chiosi et al. (1997), the same theoretical isochrones are converted to the WFPC2 photometric system, and the attention is paid to the features that isochrones and single stellar populations present in ultraviolet (UV) colours. In particular, they address the question whether the variation of UV colours of elliptical galaxies as a function of red-shift presents signatures from which one can infer the age and type of the source emitting the UV flux. Later on, Salasnich et al. (2000) present new isochrones for α-enhanced chemical mixtures, for both $UBVRIJHK$ and WFPC2 photometric systems.

The present work is a natural follow-up of this project, in which, besides extending the number of available photometric systems, we aim at updating and improving the database of stellar spectra which is at the basis of the complete procedure.

The plan of this paper is as follows: Sect. 2 details the adopted formalism. In Sect. 3, we describe the stellar spectral library in use. Sect. 4 gives the basic information about the several photometric systems under consideration. The resulting tables of bolometric corrections are then applied to a large database of stellar isochrones, which are already described in published papers and briefly recalled in Sect. 5. Sect. 6 illustrates some main properties of the derived isochrones, and describes the retrieval of data in electronic form.

2. Synthetic photometry

By synthetic photometry we mean the derivation of photometric quantities based on stellar intrinsic (and mostly theoretical) spectra, rather than on actual observations. The first works in this field (e.g. Buser & Kurucz 1978; Edvardsson & Bell 1989) were based on sets of synthetic spectra covering very modest – by present standards – intervals of effective temperature, gravity, and metallicity. The situation dramatically improved with the release of a large database of ATLAS9 synthetic spectra by Kurucz (1993). The first systematic use of Kurucz spectra on theoretical isochrones has been from Bertelli et al. (1994) and Chiosi et al. (1997).

In order to apply synthetic photometry to sets of theoretical isochrones, the basic step consists in the derivation of bolometric corrections and temperature–colour relations from the available spectra. Several papers deal with the problem (e.g. Bertelli et al. 1994; Chiosi et al. 1997; Lejeune et al. 1997; Bessell et al. 1998), presenting mathematical formalisms that, although looking somewhat different, should be equivalent and produce the same results when applied to the same sets of spectra, filters, and zero-points. In the following, we re-write this formalism in a very simple way. Our aim is to have generic formulas that, by just minimally changing their input quantities, can be applied to a wide variety of photometric systems.

2.1. Basic concepts

For a star, the spectral flux as it arrives at the Earth, f_λ, is simply related to the flux at the stellar surface, F_λ, by

$$f_\lambda = 10^{-0.4 A_\lambda} (R/d)^2 \, F_\lambda \ , \tag{1}$$

where R is the stellar radius, d is its distance, and A_λ is the extinction in magnitudes at the wavelength λ. Once f_λ is known, the apparent magnitude m_{S_λ}, in a given passband with transmission curve S_λ comprised in the interval $[\lambda_1, \lambda_2]$, is given by

$$m_{S_\lambda} = -2.5 \log \left(\frac{\int_{\lambda_1}^{\lambda_2} \lambda f_\lambda S_\lambda \mathrm{d}\lambda}{\int_{\lambda_1}^{\lambda_2} \lambda f_\lambda^0 S_\lambda \mathrm{d}\lambda} \right) + m_{S_\lambda}^0 \tag{2}$$

where f_λ^0 represents a reference spectrum (not necessarily a stellar one) that produces a known apparent magnitude $m_{S_\lambda}^0$. In other words, f_λ^0 and $m_{S_\lambda}^0$ completely define the zero-points of a synthetic photometric system (see Sect. 2.3 below).

In Eq. (2), the integrands $\lambda f_\lambda S_\lambda$ are proportional to the photon flux (i.e. number of photons by unit time, surface, and wavelength interval) at the telescope detector. This kind of integration applies well to the case of modern photometric systems that have been defined and calibrated using photon-counting devices such as CCDs and IR arrays. However, more traditional systems like the Johnson-Cousins-Glass $UBVRIJHKLMN$ one, have been defined using energy-amplifier devices. In this latter case, energy integration, i.e.

$$m_{S_\lambda} = -2.5 \log \left(\frac{\int_{\lambda_1}^{\lambda_2} f_\lambda S_\lambda \mathrm{d}\lambda}{\int_{\lambda_1}^{\lambda_2} f_\lambda^0 S_\lambda \mathrm{d}\lambda} \right) + m_{S_\lambda}^0 \ , \qquad (3)$$

would be more appropriate to recover the original system. Notice, however, that the difference between energy and photon integration is usually very small, unless the pass-bands are extremely wide. Unless otherwise stated, in papers of this series we will adopt the integration of photon counts.

2.2. Deriving bolometric corrections

The starting point of our work are extended libraries of stellar intrinsic spectra F_λ, as derived from atmosphere calculations for a grid of effective temperatures $T_{\rm eff}$, surface gravities g, and metallicities [M/H]. The particular library we adopt will be described in Sect. 3.

From this library, we aim to derive the absolute magnitudes M_{S_λ} for each star of known ($T_{\rm eff}, g,$ [M/H]) – and hence known F_λ. This can be obtained by means of Eq. (2) (or 3), once a distance of $d = 10$ pc is assumed, i.e.

$$M_{S_\lambda} = -2.5 \log \left[\left(\frac{R}{10\,\mathrm{pc}} \right)^2 \frac{\int_{\lambda_1}^{\lambda_2} \lambda F_\lambda 10^{-0.4 A_\lambda} S_\lambda \mathrm{d}\lambda}{\int_{\lambda_1}^{\lambda_2} \lambda f_\lambda^0 S_\lambda \mathrm{d}\lambda} \right] + m_{S_\lambda}^0 \qquad (4)$$

and once the stellar radius R is known. Since the quantities ($T_{\rm eff}, g,$ [M/H]) are not enough to specify R (in this case we need to have also the stellar mass M), we should first eliminate R from our equations. This is possible if we deal with the bolometric corrections,

$$BC_{S_\lambda} = M_{\rm bol} - M_{S_\lambda} \ . \qquad (5)$$

From the definition of bolometric magnitude, we have (see also Bessell et al. 1998 for a similar approach):

$$\begin{aligned} M_{\rm bol} &= M_{{\rm bol},\odot} - 2.5 \log(L/L_\odot) \qquad (6) \\ &= M_{{\rm bol},\odot} - 2.5 \log(4\pi R^2 F_{\rm bol}/L_\odot) \ , \end{aligned}$$

where $F_{\rm bol} = \int_0^\infty F_\lambda \mathrm{d}\lambda = \sigma T_{\rm eff}^4$ is the total emerging flux at the stellar surface.

Substituting Eqs. (3) and (6) into Eq. (5), we get

$$\begin{aligned} BC_{S_\lambda} &= M_{{\rm bol},\odot} - 2.5 \log \left[4\pi (10\,\mathrm{pc})^2 F_{\rm bol}/L_\odot \right] \qquad (7) \\ &\quad +2.5 \log \left(\frac{\int_{\lambda_1}^{\lambda_2} \lambda F_\lambda \, 10^{-0.4 A_\lambda} S_\lambda \mathrm{d}\lambda}{\int_{\lambda_1}^{\lambda_2} \lambda f_\lambda^0 S_\lambda \mathrm{d}\lambda} \right) - m_{S_\lambda}^0 \end{aligned}$$

that, as expected, depends only the spectral shape ($F_\lambda \, 10^{-0.4 A_\lambda}/F_{\rm bol}$), and on basic astrophysical constants.

To keep consistency with our previous works (e.g. Salasnich et al. 2000), we adopt $M_{{\rm bol},\odot} = 4.77$, and $L_\odot = 3.844 \times 10^{33}\,\mathrm{erg\,s^{-1}}$ (Bahcall et al. 1995).

By means of Eq. (7), we tabulate BC_{S_λ} for all spectra in our input library, and for several different photometric systems. The BC_{S_λ} can be then derived for any intermediate ($T_{\rm eff}, g,$ [M/H]) value, by interpolation in the existing grid. We adopt simple linear interpolations, with $\log T_{\rm eff}$, $\log g$, and [M/H] as the independent variables.

Next, to attribute absolute magnitudes to stars of given ($T_{\rm eff}, L$) along an isochrone, we simply compute $M_{\rm bol}$ with Eq. (6), and hence

$$M_{S_\lambda} = M_{\rm bol} - BC_{S_\lambda} \ . \qquad (8)$$

In this formalism, an extinction curve A_λ can be applied to all spectra of the stellar library, so as to allow the derivation of bolometric corrections (and synthetic absolute magnitudes) that already include extinction in a self-consistent way (cf. Eqs. 7 and 8). With this approach, the extinction on each pass-band depends not only on the total amount of extinction, but also on the spectral energy distribution of each star – i.e. on its spectral type, luminosity class, and metallicity (see also Grebel & Roberts 1995). Anyway, for the sake of simplicity, in the present work we will deal with the case $A_\lambda = 0$ only. Tables for different extinction curves will be discussed in a forthcoming paper.

Finally, it is worth mentioning that the newly-defined SDSS photometric system makes use of an unusual definition for magnitudes (see Lupton et al. 1999). This specific case, for which some of the above equations do not apply, will also be discussed in a subsequent paper of this series.

2.3. Reference spectra and zero-points

By photometric zero-points, one usually means the constant quantities that one should add to instrumental magnitudes in order to transform them to standard magnitudes, for each filter S_λ. In the formalism here adopted, however, we do not make use of the concept of instrumental magnitude, and hence such constants do not need to be defined. Throughout this work, instead, by "zero-points" we refer to the quantities in Eqs. (2) and (3) that depend only on the choice of f_λ^0 and $m_{S_\lambda}^0$. They are constant for each filter, and are responsible for the conversion of the synthetic magnitude scale into a standard system.

As for these quantities, there are four different cases of interest:

2.3.1. VEGAmag systems

They make use of Vega (α Lyr) as the primary calibrating star. The most famous among these systems is the Johnson-Cousins-Glass $UBVRIJHKLMN$ one, that can be accurately recovered by simply assuming that Vega has $V = 0.03$ mag, and all colours equal to 0. Other systems, like Washington and the HST/WFPC2 VEGAmag one, follow a similar definition (some colours, however, are defined to have values slightly different from 0).

Calibrated empirical spectra of Vega are available (e.g. Hayes & Latham 1975; Hayes 1985), covering the wavelength range from 3300 to 10500 Å, an interval that can be extended up to 1150 Å when complemented with IUE spectra (Bohlin et al. 1990). They can be used to define VEGAmag systems in the optical and ultraviolet.

However, as the wavelength range accessible to present instrumentation is much wider, a Vega spectrum covering the complete spectral range has become necessary. Synthetic spectra as those computed by Kurucz (1993) and Castelli & Kurucz (1994), fulfill this aim. In this case, the predicted fluxes at Vega's surface, F_λ, are scaled by the geometric dilution factor

$$(R/d)^2 = (0.5\,\theta_{\rm d}/206264.81)^2 \ , \tag{9}$$

where $\theta_{\rm d}$ is the observed Vega's angular diameter (in arcsec) corrected by limb darkening.

More recently, composite spectra of Vega have been constructed by assembling empirical and synthetic spectra together (e.g. Colina et al. 1996), so that some small deficiencies characteristic of synthetic spectra[1] are corrected. This has the precise scope of providing a reference spectrum for conversions between apparent magnitudes of real (observed) stars, and physical fluxes. However, it is not clear whether such composite Vega spectrum should be preferable when synthetic photometry is performed on theoretical spectra, as in the present work. For instance, if the ATLAS9 spectrum for Vega has the core of Balmer lines differing by as much as 10 percent from the observed ones (cf. Colina et al. 1996), it is probable that the same deviations will be present in all Kurucz spectra of comparable temperatures/gravities. If this is the case, the synthetic Vega spectrum would probably give better zero-points for these stars than the composite Colina et al. (1996) one.

For this reason, we simply adopt the synthetic ATLAS9 model for Vega, with $T_{\rm eff} = 9550$ K, $\log g = 3.95$, [M/H] $= -0.5$, and microturbulent velocity $\xi = 2\,{\rm km\,s^{-1}}$, the spectrum being provided by Kurucz (1993). Castelli & Kurucz (1994) have computed a higher-resolution spectrum for the same model, using the more refined ATLAS12 code. As discussed by these authors, ATLAS9 and ATLAS12 spectra for Vega are almost identical.

Once the synthetic model $F_\lambda^{\rm Vega}$ is chosen, we just need to adopt a fixed value for the dilution factor $(R/d)^2$, in order to have $f_\lambda^{\rm Vega}$ at the Earth's surface (outside the atmosphere). Two choices are possible then: We either (i) adopt an observed value of $\theta_{\rm d}$ as input to Eq. (9), or (ii) adopt the observed Vega flux as measured at the stellar surface, at a given wavelength, as an input to Eq. (1).

Since direct measures of $\theta_{\rm d}$ are relatively more uncertain than direct measures of $f_\lambda^{\rm Vega}$, we prefer to adopt the second alternative: Taking the flux values at 5556 Å from Hayes (1985; $f_\nu^{\rm Vega} = 3.542 \times 10^{-20}$ ${\rm erg\,s^{-1}\,cm^{-2}\,Hz^{-1}}$), and at 5550 Å from Kurucz (1993) Vega model ($F_\lambda^{\rm Vega} = 5.507 \times 10^7\,{\rm erg\,s^{-1}\,cm^{-2}\,Å^{-1}}$), we obtain $(R/d)^2 = 6.247 \times 10^{-17}$. This value implies an angular diameter of $\theta_{\rm d} = 3.26$ mas (Eq. 9) for Vega, that compares very well with the observed values of 3.24 ± 0.07 mas (Code et al. 1976) and 3.28 ± 0.06 mas (Ciardi et al. 2000).

[1] For a discussion of the differences between synthetic and observed Vega spectra, the reader is referred to Castelli & Kurucz (1994) and Colina et al. (1996).

It is worth remarking that, since the zero-points in VEGAmag systems are attached to the observed Vega fluxes, their synthetic absolute magnitudes may have systematic errors of a few hundredths of magnitude (say up to 0.03 mag), which is the typical magnitude of errors in measuring fluxes at the Earth's surface. Somewhat smaller errors, however, are expected in the colours. These uncertainties will probably not be eliminated unless definitive $\theta_{\rm d}$ and $f_\lambda^{\rm Vega}$ measurements become available.

2.3.2. ABmag systems

In the original work by Oke (1964), monochromatic AB magnitudes are defined by

$$m_{{\rm AB},\nu} = -2.5\,\log f_\nu - 48.60 \ . \tag{10}$$

This means that a reference spectrum of constant flux density per unit frequency

$$f^0_{{\rm AB},\nu} = 3.631 \times 10^{-20}\ \ {\rm erg\,s^{-1}\,cm^{-2}\,Hz^{-1}} \tag{11}$$

will have AB magnitudes $m^0_{{\rm AB},\nu} = 0$ at all frequencies ν.

This definition can be extended to any filter system, provided that we replace the monochromatic flux f_ν with the photon counts over each pass-band S_λ obtained from the star, compared to the photon counts that one would get by observing $f^0_{{\rm AB},\nu}$:

$$m_{{\rm AB},S_\lambda} = -2.5\,\log\left[\frac{\int_{\lambda_1}^{\lambda_2}(\lambda/hc) f_\lambda S_\lambda {\rm d}\lambda}{\int_{\lambda_1}^{\lambda_2}(\lambda/hc) f^0_{{\rm AB},\lambda} S_\lambda {\rm d}\lambda}\right] \ , \tag{12}$$

where $f^0_{{\rm AB},\lambda} = f^0_{{\rm AB},\nu}\,c/\lambda^2$. Then, it is easy to show that Eq. (12) is is just a particular case of our former Eq. (2), for which $f^0_{{\rm AB},\nu}$ is the reference spectrum, and $m^0_{{\rm AB},S_\lambda} = 0$ are the reference magnitudes.

It is worth mentioning that different practical implementations of the ABmag system have been defined over the years (e.g. Oke & Gunn 1979, and Fukugita et al. 1996). They differ only in the definition of the reference stars (or reference stellar spectra) used as spectrophotometric standards during the conversion from *observed* instrumental magnitudes into fluxes f_ν (that are used in Eq. 10). Since we are dealing with synthetic spectra only, such a conversion is not necessary in our case. It follows that these different definitions are not a point of concern to us.

2.3.3. STmag systems

ST monochromatic magnitudes have been introduced by the HST team, and are defined by

$$m_{{\rm ST},\lambda} = -2.5\,\log f_\lambda - 21.10 \ . \tag{13}$$

This means that a reference spectrum of constant flux density per unit wavelength

$$f^0_{{\rm ST},\lambda} = 3.631 \times 10^{-9}\ \ {\rm erg\,s^{-1}\,cm^{-2}\,Å^{-1}} \tag{14}$$

will have ST magnitudes $m^0_{\mathrm{ST},\lambda} = 0$ at all wavelengths. Similarly to the case of AB magnitudes, this can be generalized to any pass-band system with:

$$m_{\mathrm{ST},S_\lambda} = -2.5 \log \left[\frac{\int_{\lambda_1}^{\lambda_2} (\lambda/hc) f_\lambda S_\lambda \mathrm{d}\lambda}{\int_{\lambda_1}^{\lambda_2} (\lambda/hc) f^0_{\mathrm{ST},\lambda} S_\lambda \mathrm{d}\lambda} \right] . \quad (15)$$

Again, this situation is easily reproduced in our formalism with the adoption of $f^0_\lambda = f^0_{\mathrm{ST},\lambda}$ and $m^0_{\mathrm{ST},S_\lambda} = 0$.

2.3.4. "Standard stars" systems

This class comprises all photometric systems that use standard stars different from Vega to define the zero-points. Good examples are the Vilnius (Straizys & Zdanavicius 1965) and Thuan-Gunn (Thuan & Gunn 1976) systems.

In this case, we are forced to use empirical spectra of standard stars in order to define f^0_λ and $m^0_{S_\lambda}$. A good set is provided by the four metal-poor subdwarfs BD +17°4708, BD+26°2606, HD 19445 and HD 84937, which are widely-used spectrophotometric secondary standards (Oke & Gunn 1983), as well as standards for several photometric systems.

Actually, the present work does not deal with any "standard stars" system, and this case is here included just for the sake of completeness. Details about a few specific systems – including the possible choices for f^0_λ – will be given in forthcoming papers.

3. The stellar spectral library

In the following, we will present the stellar spectral library put together for this work. For the sake of reference, Fig. 1 presents the distribution of all spectra in the $\log T_{\mathrm{eff}} - \log g$ plane.

3.1. Kurucz atmospheres

Earlier Padova isochrones were based on the Kurucz (1993) libraries of ATLAS9 synthetic atmospheres. As discussed in a series of papers by Castelli et al. (1997), Bessell et al. (1998), and Castelli (1999), these models are superseded by now. Firstly, small discontinuities associated to the scheme of "approximate overshooting" initially adopted by Kurucz have been corrected (cf. Bessell et al. 1998). Secondly, no-overshooting models have been demonstrated to produce T_{eff}-colour relations in better agreement with empirical ones, at least for stars hotter than the Sun (Castelli et al. 1997).

3.1.1. The more recent models

In the present work, we adopt the ATLAS9 no-overshoot models that have been calculated by Castelli et al. (1997). They correspond to the "NOVER" files available at `http://cfaku5.harvard.edu/grids.html`. The metallicities cover the values [M/H] = −2.5, −2.0, −1.5, −1.0, −0.5, 0.0, and +0.5, with solar-scaled abundance ratios. A microturbulent velocity $\xi = 2\,\mathrm{km\,s^{-1}}$, and a mixing length parameter $\alpha = 1.25$, are adopted. Notice that these models are now being extended so as to include also α-enhanced chemical mixtures, which represents a potentially important improvement for our future works.

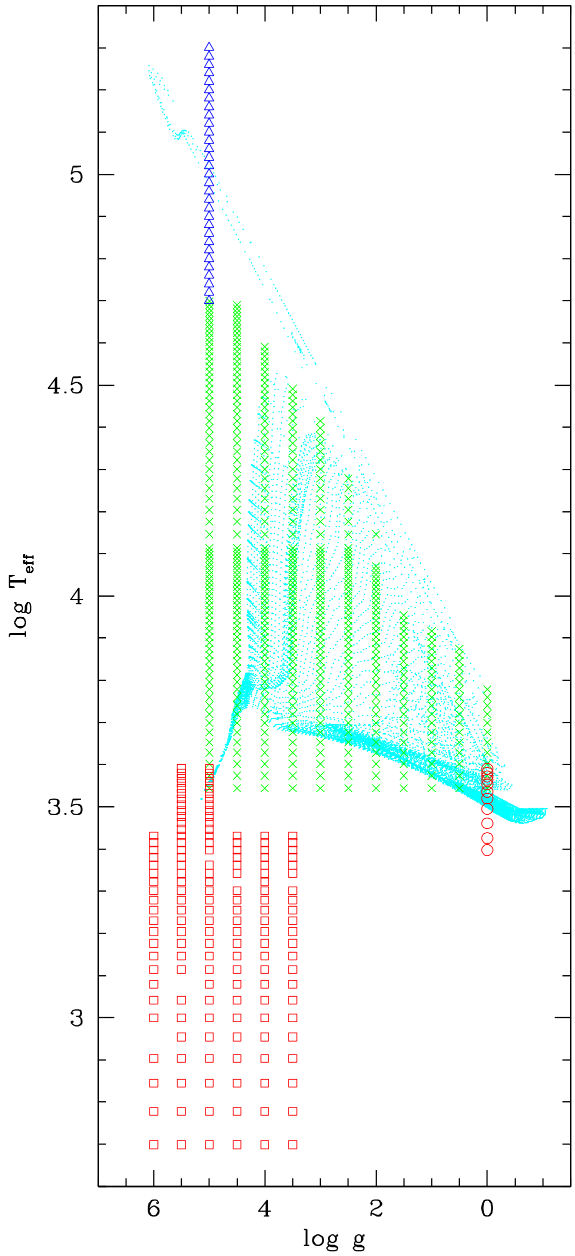

Fig. 1. Distribution of the [M/H] = 0 spectra incorporated in our stellar library (large symbols) in the $\log T_{\mathrm{eff}} - \log g$ plane, compared to the position of stellar models of solar metallicity (small dots; these models are isochrones to be discussed later in Sect. 5.1). The spectra are taken from Castelli et al. (1997; crosses), Fluks et al. (1994; circles), Allard et al. (2000a; squares), and pure blackbody (triangles). Fluks et al. spectra have been arbitrarily located at $\log g = 0$. Similar distributions hold for all metallicities between [M/H] = −2.5 and +0.5 (see text).

Kurucz models cover quite well the region of the $\log T_{\rm eff}$ vs. $\log g$ plane actually occupied by stars, at least in the $3500\,{\rm K} \le T \le 50\,000\,{\rm K}$, $0 \le \log g \le 5$ intervals (see Fig. 1). However, it has to be extended to both lower and higher $T_{\rm eff}$s, as will be detailed below.

It is important to recall that Kurucz (ATLAS9) spectra are widely used in the field of synthetic photometry, mainly because of their wide coverage of stellar parameters and easy availability. Moreover, there are also good indications in the literature that these spectra do a good job in synthetic photometry, provided that we are dealing with broad-band systems. Compelling examples of this can be found in Bessell et al. (1998), who compares the $UBVRIJHKL$ results obtained from the recent ATLAS9 spectra to empirical relations derived with the infrared flux method, lunar occultations, interferometry, and eclipsing binaries. Their results indicate that the 1998 ATLAS9 models are well suited to synthetic photometry, but for small errors, generally lower than 0.1 mag in colours, that we do not consider as critical. In fact, we are more interested in the overall dependencies of colours and magnitudes with stellar parameters – probably well represented by present synthetic spectra – than on details of this order of magnitude.

Additionally, Worthey (1994) presented extensive comparisons between Kurucz (1993) spectra and stars in the low-resolution spectral library by Gunn & Stryker (1983), obtaining generally a good match for wavelengths redder than the B pass-band. Worthey's figure 9 also presents a comparison between Kurucz (1993) solar spectra and Neckel & Labs (1984) data, with excellent results (errors lower than 0.1 mag) all the way from the UV up to the near-IR. Since the ATLAS9 1998 spectra differ just little from the Kurucz (1993) version (a few percent in extreme cases), these results are to be considered still valid.

3.1.2. Some caveats on ATLAS9 spectra

The previously mentioned works point to a reasonably good agreement between ATLAS9 spectra and those of real stars of near-solar metallicity, especially in the visual and near-infrared pass-bands. However, there are many known inadequacies in these spectra, which should be kept in mind as well. Here, we give just a brief list of the potential problems, concentrating on those which may be more affecting our synthetic colours.

ATLAS9 spectra are based on 1D static and plan-parallel LTE model atmospheres, which use a huge database of atomic line data (Kurucz 1995). The line list is known not to be accurate: In fact, Bell et al. (1994) show that the solar spectra calculated using Kurucz list of atomic data present many unobserved lines; moreover, the number of lines which are too strong exceeds those which are too weak. The problem can be appreciated by looking at the high-resolution spectral plots presented by Bell et al. (1994), but could hardly be noticeable in low-resolution plots (such as in the comparisons presented in Worthey's 1994 figure 9, and in Castelli et al. 1997 figure 2).

Also, Bell et al. (2001) show that a motivated increase in the Fe I bound-free opacity cause a significant improvement in the fitting of the solar spectrum in the $3000-4000$ Å wavelength region, affecting the entire UV region as well. Such increased sources of continuous opacity are still missing in ATLAS9 atmospheres[2].

These results indicate that ATLAS9 spectra will produce worse results when applied to (i) narrow-band photometric systems, in which individual metallic lines can more significantly affect the colours, and (ii) in the UV region, especially shortward of 2720 Å (see Bell et al. 2001). In both cases, the errors caused by wrong atomica data are such that we can expect not only systematic and $T_{\rm eff}$-dependent offsets in synthetic colours, but also a somewhat wrong dependence on metallicity. Clearly, these points are worth being properly investigated by means of detailed spectral comparisons.

Regarding the present work, the above-mentioned problems (i) critically determine the inadequacy of synthetic colours computed for the Strömgren system (Girardi et al., in preparation), and (ii) may possibly cause significant errors in our synthetic HST/WFPC2 UV colours.

Other potential problems worth of mention are:

- The deficiencies in 1D atmosphere models and in the mixing length description of convection, as compared to exploratory 3D model atmospheres (e.g. Asplund et al. 2000). They should affect mainly the intermediate-strong lines with significant non-thermal broadening and in stars cooler than ~ 6000 K. The consequences of spatial and thermal inhomogeneities in the atmosphere of the Sun and Procyon have been investigated by Allende Prieto et al. (2001, 2002).
- Inadequacies in the hydrogen line computations. Especially affected are high members of the Balmer series in GK stars – due to inhomogeneities in real atmospheres and inadequate treatment of hydrogen line broadening in cool stars (see Barklem et al. 2000a,b) – and the core of Balmer lines and the region around the Paschen discontinuity and longward in A stars (Colina et al. 1996). In synthetic photometry, these inadequacies are expected to slightly affect the U and B magnitudes for A-F stars, but to have a greater effect in Strömgren indices.
- The inadequacy of using scaled-solar metal ratios in giants where the abundance of CNO elements has been altered by dredge-up events. Similarly, the inadequancy of using scaled-solar abundances for halo and bulge stars, instead of α-enhanced ones.

Obviously, some improvement upon these points is expected in future releases of ATLAS spectra (see Castelli

[2] In the original Kurucz (1993) spectra, a modest reduction of the continuous UV flux results from the adopted "approximate overshooting" scheme.

& Kurucz 2001), and of other extended spectral grids as well. Fortunately, the work by Bessell et al. (1998) gives us some confidence that present broad-band magnitudes and colours (from U to K) are modelled with an accuracy that is already acceptable for many applications.

Finally, we remark that some authors (Lejeune et al. 1997, 1998) propose the application of *a posteriori* transformations to Kurucz (1993) spectra, as a function of wavelength and $T_{\rm eff}$, such as to reduce the errors of the derived synthetic $UBVRIJHKL$ photometry. In our opinion, such transformations are questionable because they do not correct the cause of the discrepancies – majorly identifiable in the imperfect modelling of absorption lines – and the case for applying them to stars of all surface metallicities and gravities is far from compelling.

3.2. Extension to higher temperatures

For $T_{\rm eff} > 50\,000$ K, we simply assume black-body spectra. This is probably a good approximation for wavelengths $\lambda > 912$ Å. In fact, we find always a reasonably smooth transition in the computed BC_{S_λ}s as we cross the $T_{\rm eff} = 50\,000$ K temperature boundary.

3.3. Extension to M giants

Synthetic spectra for M giants have still many problems – mainly in their ultraviolet-blue region – that partially derive from incomplete opacity lists of molecules such as TiO, VO and H_2O (see e.g. Plez 1999; Alvarez & Plez 1998; Alvarez et al. 2000; and Houdashelt et al. 2000a,b to appreciate the state of the art in the field).

Therefore, we prefer to use the empirical M giant spectra from Fluks et al. (1994; or "intrinsic" spectra as referred in their paper). They cover the wavelength interval from 3800 Å to 9000 Å. Outside this interval, the empirical spectra have been extendend with the "best fit" synthetic spectra computed by the same authors.

However, the whole procedure reveals a problem: if we simply merge empirical and synthetic spectra from Fluks et al. (1994), the resulting synthetic $B-V$ and $U-B$ colours just badly correlate with the measured colours for the same stars (which were also obtained by Fluks et al. 1994). This problem probably derives from a bad flux calibration at the blue extremity of the observed spectra and/or from the imperfect match between synthetic and observed spectra at 3800 Å. In order to circumvent (at least partially) the problem, we simply multiply each M-giant spectrum blueward of 4000 Å (with a smooth transition in the range from 4000 Å to 4800 Å) by a constant, typically between 0.8 and 1.2, so that the synthetic colours recover the observed behaviour of the $B-V$ vs. $V-K$ data. The first two panels of Fig. 2 show the results.

Actually, Fig. 2 presents six different colour vs. $V-K$ diagrams that are useful to understand the situation for giants. Care has been taken in expressing data and models in the same photometric system, the "Bessell" $UBVRIJHK$ one, that we will detail later in Sect. 4.1. For M giants, the empirical photometric data from Fluks et al. (1994; small dots) can be compared with the results of our synthetic photometry[3]. Noteworthy, there is a reasonably good match between the synthetic and observed relations for most colours. This has been imposed for $U-B$ and $B-V$, whereas is a natural result for all colours involving wavelengths longer than ~ 4800 Å. The only clear exception is the $V-R$ colour, for which differences of ~ 0.4 mag are found for all giants of spectral type later than M4 ($V-K \gtrsim 5$). The reason for this discrepancy is not clear, but may lie in the use of R filters with different transmission curves. Also the predictions for $J-K$ do not fit well all the photometric data, somewhat failing for the spectral types later than M7 ($V-K \gtrsim 8$). However, since these latters are quite rare, such mismatch does not pose a serious problem.

For the sake of comparison, Fig. 2 also presents the relations obtained by means of the M-giant models from Houdashelt et al. (2000a), in the case of solar metallicity. Together with other recent examples (e.g. Plez 1999; Alvarez et al. 2000), they represent state-of-the-art computations of cool oxygen-rich stellar atmospheres. As can be appreciated in the figure, Houdashelt et al. models reproduce well the empirical data as far as $V-K \lesssim 6$ (spectral types earlier than M5), but start departing from these for cooler stars. A similar situation holds if we look at different $T_{\rm eff}$–colour relations, as can be seen in figures 13 and 14 of Houdashelt et al. (2000a), where they compare their $T_{\rm eff}$–colour relations with those obtained with Fluks et al. (1994) spectra and data for field giants. Also in this case, it seems that Fluks et al. (1994) spectra do better reproduce the empirical relations for the spectral types later than M4.

Once we have defined the library of M-giant spectra, we associate effective temperatures to them by using the scale favoured by Fluks et al. (1994). In this scale, M giants cover the temperature interval from 3 850 K (MK type M0) to 2 500 K (MK type M10). We recall that Fluks et al. (1994) $T_{\rm eff}$ values are derived from a careful fitting of the observed spectra with synthetic model atmospheres of solar metallicity. Their scale is also in excellent agreement with the empirical one from Ridgway et al. (1980), which covers spectral types earlier than M6.

After the proper $T_{\rm eff}$ is attributed, each one of our modified spectra is completely re-scaled by a constant, so that the total flux vs. $T_{\rm eff}$ relation – i.e. $F_{\rm bol} = \sigma T_{\rm eff}^4$ – is recovered.

Finally, we face the problem of defining the transition between the M-giant spectra, and the ATLAS9 ones which are available for temperatures higher than 3 500 K. To this aim, it is helpful to examine Fig. 2, where we also include:

[3] The JHK colours from Fluks et al. are in the ESO system and have been converted to the Bessell one by using the relations found in Bessell & Brett (1988).

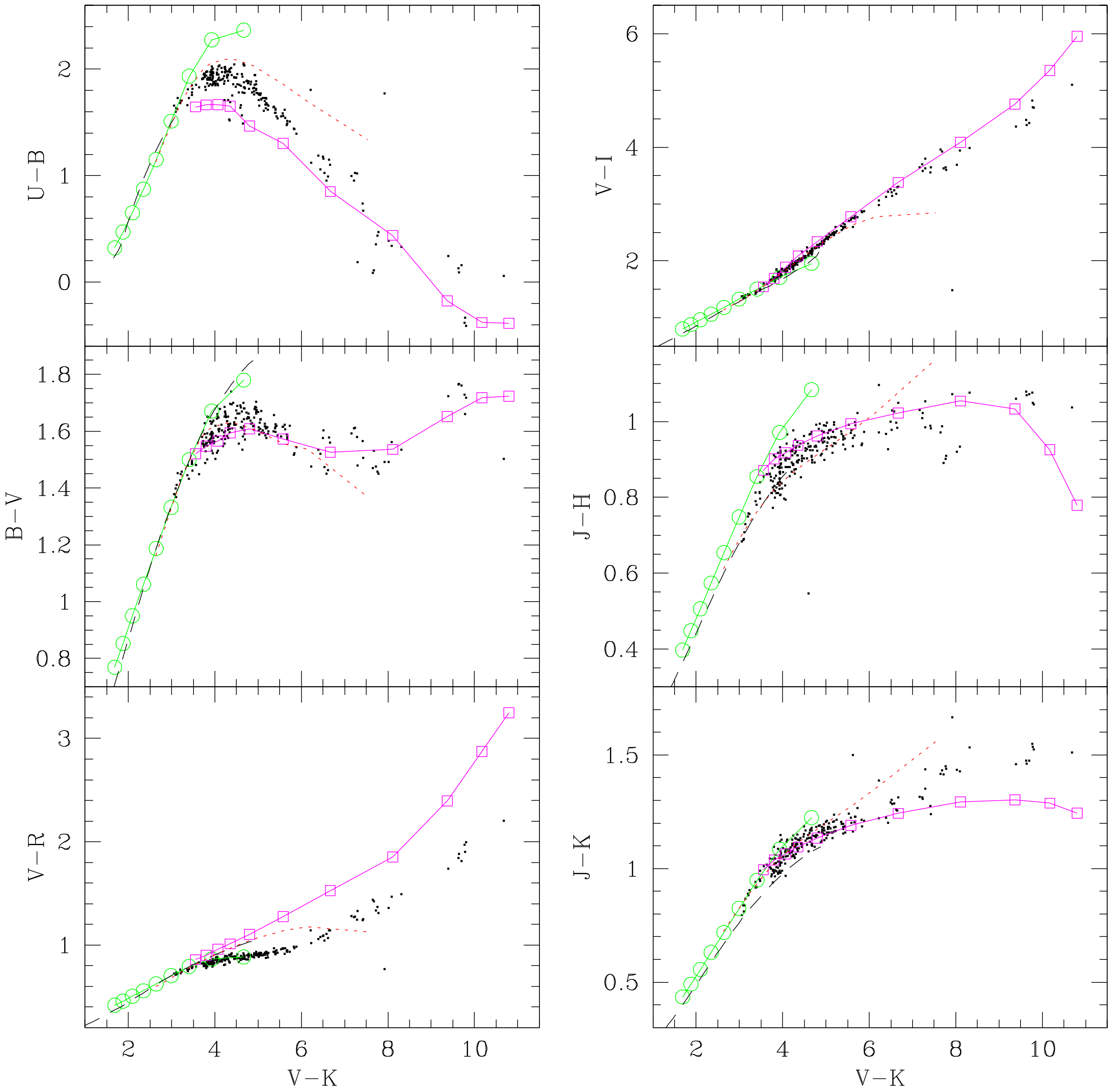

Fig. 2. Colour vs. $V-K$ relations for giants. The connected open circles represent the relation obtained from [M/H] = 0 ATLAS9 spectra located along the $T_{\rm eff} = 3250 + 500 \log g$ line (the typical location for RGB stars) in the diagram of Fig. 1. The connected open squares correspond to the relation obtained from the M-giant spectra from Fluks et al. (1994), completed and modified at $\lambda < 4800$ Å as detailed in the text. The dashed lines represent the empirical relations for F0–K5 solar-metallicity giants from Alonso et al. (1999b), whereas the dotted lines are the synthetic relations for K0–M7 giants from Houdashelt et al. 2000a). The empirical data for M giants (small dots) are from Fluks et al. (1994). As far as possible, all observations have been converted to the same photometric system as used in our synthetic photometry (i.e. the "Bessell" $UBVRIJHK$ system; see text).

– the synthetic photometry for a sequence of ATLAS9 spectra for M giants (empty circles). These spectra are located along the line $T_{\rm eff} = 3250 + 500 \log g$, which represents fairly well the locus of low-mass red giants in a $T_{\rm eff}$ vs. $\log g$ diagram (see Fig. 1).

– the mean empirical relations for F0–K5 giants of [Fe/H] = 0 as derived from Alonso et al. (1999b) fitting formulas (dashed lines)[4].

[4] Alonso et al. (1999b) $V-I$ and $V-R$ colours have been transformed from Johnson to Johnson-Cousins systems using relations from Bessell (1979), whereas infrared colours were

An important fact to be noticed is that our synthetic photometry reproduces Alonso et al. (1999b) relations in all colours remarkably well.

From inspecting this and other similar plots, we can conclude that the mismatch between Kurucz ATLAS9 and Fluks et al. (1994) spectra starts at about $T_{\rm eff} = 3\,850$ and increases slowly as the temperature decreases down to 3 500 K (i.e. from $V-K \simeq 3.5$ to $V-K \simeq 4.7$). Hence, we adopt a smooth transition between these two spectral sources over this temperature interval. The same M giant spectra are assumed for all metallicities.

The complete procedure ensures reasonable colour vs. $V-K$ relations for all giants of near-solar metallicity (Fig. 2). Nevertheless, this kind of approach cannot be completely satisfactory, first because the original Fluks et al. (1994) spectra have been artificially corrected at wavelengths shorter than 4800 Å in order to produce reasonable $B-V$ and $U-B$, and second because we do not dispose of similar M-giant spectra for metallicities very different from solar. Better empirical and theoretical spectra for M giants seem to be urgently needed. Anyway, in the context of the present work the problem is not dramatic because M giants cooler than $T_{\rm eff} \sim 3\,500$ K are only found in the RGB-tip and TP-AGB phases of high metallicity stellar populations, and constitute just a tiny fraction of the number of red giants. The problem could be critical, instead, when we consider integrated properties of stellar populations, because M giants, despite their small numbers, have high luminosities and contribute a sizeable fraction of the integrated light.

3.4. Extension to M+L+T dwarfs

Although the modelling of cool dwarfs atmospheres presents challenges comparable to those found in late-M giants (e.g. the inadequacy of TiO and H_2O line lists, and dust formation; see Tsuji et al. 1996, 1999; Leggett et al. 2000), present results compare reasonably well with observational spectral data (see e.g. figure 9 in both Leggett et al. 2000 and 2001). A review on the subject can be found in Allard et al. (1997).

An extended library of synthetic spectra for cool dwarfs (of types M and later) is provided by Allard et al. (2000a; see `ftp://ftp.ens-Lyon.fr/pub/users/CRAL/fallard`). We use their set of "BDdusty1999" atmospheres (see also Chabrier et al. 2000; Allard et al. 2000b, 2001), that should supersede the "NextGen" models from the same group (Hauschildt et al. 1999) due to the consideration of better opacity lists and dust formation. Dust can significantly affect the coolest atmospheres, corresponding to dwarfs of spectral types L and T.

The selected spectra cover the $T_{\rm eff}$ intervals:

- from 4 000 K to 2 800 K ("AMES" models) for metallicities [M/H] = 0.0, −0.5, −1.0, −1.5, and both $\log g = 5.0$ and 5.5;
- from 2 800 K down to 500 K ("AMES-dusty" models) only for [M/H] = 0.0, and $\log g$ values between 3.5 and 6.0.

These spectra are presented with a extremely high resolution, that by far exceeds the one necessary in our work. Thus, we have convolved the flux per unit frequency F_ν with a Gaussian filter of $\sigma_\nu = 2.4 \times 10^{-18}$ Hz, that corresponds to a FWHM of 20 Å at $\lambda = 5550$ Å. The resulting spectra were then reported to the same grid of wavelengths of Kurucz' spectra.

We find that there is a good agreement between ATLAS9 and BDdusty1999 spectra in the $T_{\rm eff}$ range between $\sim 3\,800$ K and 4 000 K. Then, we set the transition between ATLAS9 and BDdusty1999 spectra at $\sim 3\,900$ K. This choice guarantees smooth $T_{\rm eff}$ vs. colour relations for dwarfs.

4. Photometric systems available

In this section we present the basic information regarding the filter transmission curves and zero-points for each photometric system. As a reference to the discussion, Fig. 3 presents the filter sets under consideration, as compared to the spectra of a hot (Vega), an intermediate (the Sun), and a cool star (an M5 giant).

4.1. Johnson-Cousins-Glass system

Aiming to reproduce the Johnson-Cousins-Glass system, we adopt the filter pass-bands indicated by Bessell (1990; for Johnson-Cousins $UBVRI$) and Bessell & Brett (1988; for JHK). We also apply their prescription for computing the $U-B$ colour by means of a slightly modified pass-band BX_{90}, instead of the normal B one. Moreover, in order to better recover the original system, we adopt energy instead of photon count integrations (see Sect. 2.1).

It is worth recalling that these pass-bands represent just one specific version of the "standard" Johnson-Cousins-Glass system, that may differ from filter systems in usage at several observatories. The Bessell & Brett (1988) $JHKLM$ pass-bands, for instance, represent an effort in the direction of homogenizing several different near-infrared systems (SAAO, ESO, CIT/CTIO, MSO, AAO, and Arizona). In Bessell (1990) and Bessell & Brett (1988), the reader can find a set of useful fitting relations between colours in the several original systems.

As previously mentioned, Johnson-Cousins-Glass is essentially a VEGAmag system. We fix the zero-points by assuming that Vega has apparent magnitudes equal to 0.03 in all $UBVRIJHK$ bands, i.e. we impose all colours to be null. Notice that our definition is very similar to the Bessell et al. (1998) one, who adopt Vega colours differing from zero by just some thousandths of a magnitude (see their table A1).

converted from TCS to "Bessell" systems using the relations from Alonso et al. (1998).

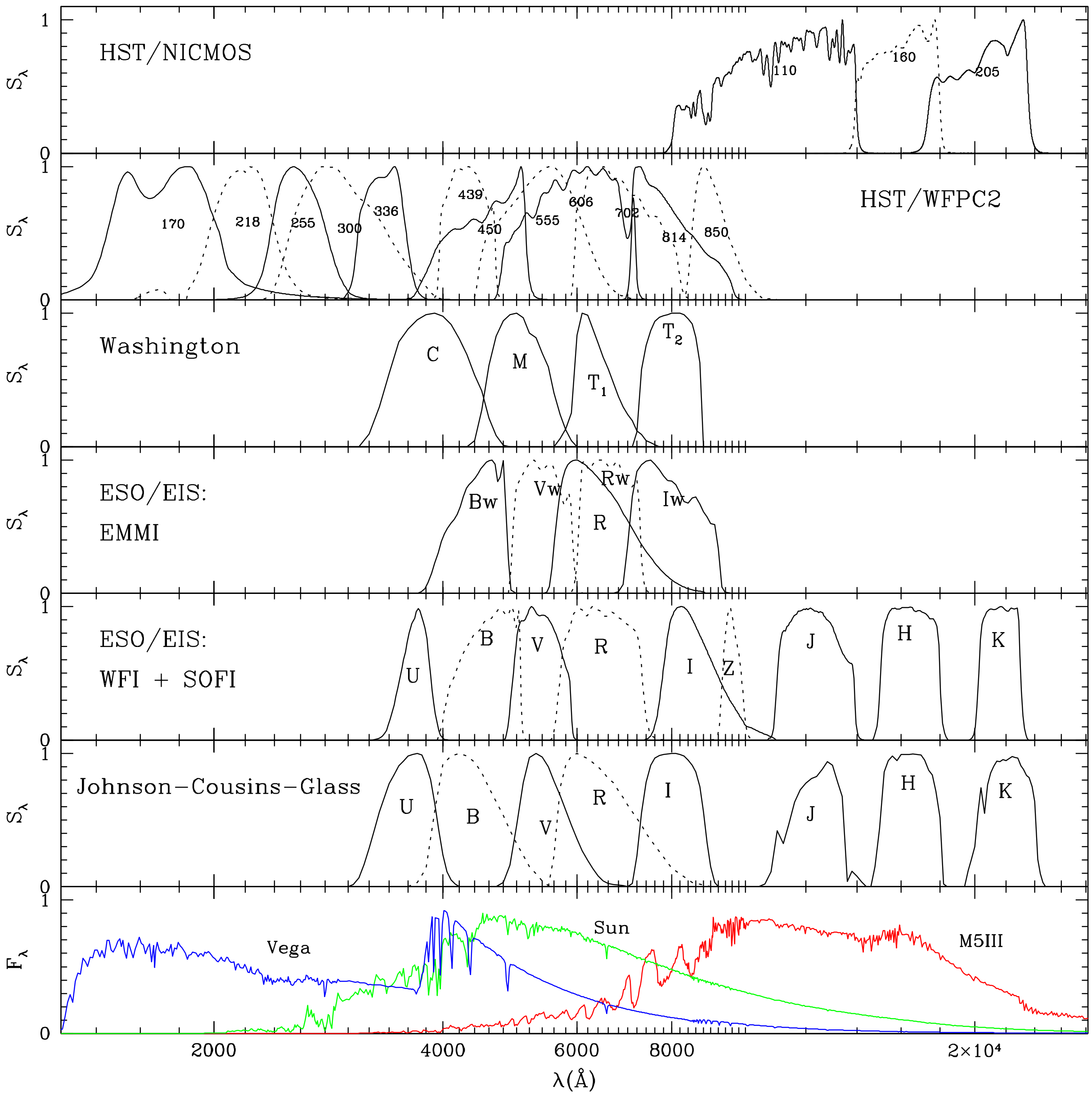

Fig. 3. The filter sets used in the present work. From top to bottom, we show the filter+detector transmission curves S_λ for the systems: (1) HST/NICMOS, (2) HST/WFPC2, (3) Washington, (4) ESO/EMMI, (5) ESO/WFI $UBVRIZ$ + ESO/SOFI JHK, and (6) Johnson-Cousins-Glass. All references are given in Sect. 4. To allow a good visualisation of the filter curves, they have been re-normalized to their maximum value of S_λ. For the sake of comparison, the bottom panel presents the spectra of Vega (A0V), the Sun (G2V), and a M5 giant, in arbitrary scales of F_λ.

4.2. Instruments on board of HST

In the context of the present work, the distinctive feature of HST photometry is the use of ABmag and STmag systems, which greatly simplifies the definition of zero-points. WFPC2 and NICMOS observations can also be expressed in VEGAmag magnitudes.

4.2.1. WFPC2

As for the WFPC2, we produce bolometric corrections and magnitudes in the F170W, F218W, F255W, F300W, F336W, F439W, F450W, F555W, F606W, F702W, F814W, and F850LP filters. Similar tables have been produced in previous papers (Chiosi et al. 1997; Salasnich et al. 2000); the present ones differ just in minor details.

The transformations have been computed in STmag, ABmag, and VEGAmag systems. Whereas the STmag and ABmag systems can be straightforwardly simulated, the VEGAmag one deserves some comments.

According to the SYNPHOT package distributed with the STSDAS software, in a VEGAmag system Vega should have apparent magnitudes equal to zero in all pass-bands. However, the most widely used calibration of WFPC2 photometry comes from Holtzman et al. (1995), who adopt a set of zero-points in which Vega has apparent magnitudes $U = 0.02$, $B = 0.02$, $V = 0.03$, $R = 0.039$, $I = 0.035$. Accordingly, we choose this latter definition, and impose that for the WFPC2 filters that correspond to $UBVRI$ in wavelength, the synthetic magnitudes of Vega have these same values. For filters of intermediate wavelength, we adopt a linear interpolation between these values, whereas for bluer and redder filters a Vega magnitude equal to zero is assumed.

As for the S_λ functions, we use the pre-launch pass-bands kindly provided by Jon Holtzman (see Holtzman et al. 1995). We recall that, owing to the presence of contaminants inside the WFPC2 (see Baggett & Gonzaga 1998; Holtzman et al. 1995), S_λ changes slowly with time, especially for UV filters. To cope with this, observers usually apply small corrections to the definition of the instrumental magnitudes, in order to bring the magnitudes back to the original conditions (see Holtzman et al. 1995). This justifies our use of pre-launch pass-bands instead of the present-day ones provided by SYNPHOT.

4.2.2. NICMOS

For NICMOS filters, we compute bolometric corrections and absolute magnitudes in the ABmag, STmag, and VEGAmag systems. For the moment, calculations are limited to the three most frequently used filters, i.e. F110W, F160W, and F205W. The pass-bands come from SYNPHOT, and have been kindly provided by Don Figer.

NICMOS observations are also frequently expressed in units of milli-Jansky (mJy). The conversion between AB magnitudes and mJy is straightforward:

$$m_{\mathrm{AB},\nu}(\mathrm{mag}) = -2.5 \log f_\nu(\mathrm{mJy}) - 16.4 \ . \qquad (16)$$

4.3. ESO Imaging Survey (EIS) filter sets

The EIS survey (Renzini & da Costa 1997; da Costa 2000) aims at providing a large database of deep photometric data, among which the astronomical community could select interesting targets for VLT spectroscopy. The survey is conducted at several different instruments at ESO:

4.3.1. WFI

The Wide Field Imager (WFI) at the MPG/ESO 2.2m La Silla telescope provides imaging of excellent quality over a $34' \times 33'$ field of view. It contains a peculiar set of broad-band filters, very different from the "standard" Johnson-Cousins ones. This can be appreciated in Fig. 3; notice in particular the particular shapes of the WFI B and I filters. Moreover, EIS makes use of the WFI Z filter which does not have a correspondency in the Johnson-Cousins system.

Given the very unusual set of filters, the importance of computing isochrones specific for WFI is evident. This has benn done so for the broad WFI filters U (ESO#841), B (ESO#842), V (ESO#843), R (ESO#844), I (ESO#845), and Z (ESO#846), that – here and in Fig. 3 – are referred to as $UBVRIZ$ for short.

Bolometric corrections have been computed in the VEGAmag system assuming all Vega apparent magnitudes to be 0.03, and in the ABmag system, which is adopted by the EIS group. The photometric calibration of EIS data is discussed in Arnouts et al. (2001).

It is very important to notice that any photometric observation performed with WFI that makes use of standard stars (e.g. Landolt 1992) to convert WFI instrumental magnitudes to the standard Johnson-Cousins $UBVRI$ system, *will not be in the WFI VEGAmag system we are dealing with here*. Instead, in that case, we should better compare the observations with the isochrones in the standard Johnson-Cousins system, or, alternatively, apply colour transformations to our WFI isochrones so that they reproduce the T_{eff}-colour sequences of dwarfs and giants in the Johnson-Cousins system. This aspect will be better illustrated Sect. 6.

4.3.2. SOFI

SOFI is a near-infrared imager and grism spectrograph at the ESO NTT 3.6m telescope. It is used to complement WFI observations in near-infrared pass-bands. More specifically, it disposes of J, H and K_{s} filters that have some similarity to Glass JHK (see Fig. 3).

VEGAmag magnitudes are computed assuming the same as before, i.e. that Vega apparent magnitudes are 0.03.

4.3.3. EMMI

EMMI is a visual imager and grism spectrograph also at the NTT. The EIS project uses a set of its wide filters, i.e. B_{w}, I_{w}, R_{w}, and V_{w}, together with the R filter. The pass-bands have been kindly provided by S. Arnouts. As before, VEGAmag magnitudes are computed assuming that Vega has 0.03 mag in all filters.

4.4. Washington system

The Washington system, originally defined by G. Wallerstein and developed by Canterna (1976), has been more and more used since Geisler (1996) defined a set of CCD standard fields. In the present paper, we reproduce the Washington CCD system (filters C, M, T_1 and T_2)

by adopting the transmission curves as revised by Bessell (2001).

Following Geisler (1996), the Washington T_1 filter has been frequently replaced by the Kron-Cousins filter R, which presents a similar transmission curve and is available in almost all observatories. Additionally, Holtzman et al. (in preparation) suggest the use of BVI colours together with Washington ones for breaking the age-metallicity degeneracy of stellar populations in colour-colour diagrams. For these reasons, in all tables that deal with the Washington CMT_1T_2 system, we also insert the information for the Johnson-Cousins $BVRI$ filters.

Finally, following Geisler (private communication), the zero-points should be well represented by a VEGAmag system. We assume Vega has magnitude 0.03 in all filters.

4.5. Other planned systems

Forthcoming papers of this series will be dedicated to

- other traditional systems like Strömgren, Thuan-Gunn, Vilnius, etc.;
- systems corresponding to some successful and recent/ongoing observational campaigns, like Hipparcos, MACHO, DENIS, 2MASS, and SDSS;
- newly-proposed systems, like the ones for the future astrometric mission GAIA.

Since the procedure for computing BC_{S_λ} tables is relatively easy, provided the necessary information – i.e. filter transmission curves and a zero-point definition that corresponds to one of the cases discussed in Sect. 2.3 – is given, we can provide isochrone tables for any photometric systems upon request.

5. Available stellar tracks and isochrones

The tables of bolometric corrections here described have been primarily constructed to be applied to the Padova database of stellar evolutionary tracks and isochrones[5]. These latter have been described in several previous papers, and a complete description of them is beyond the scope of this work.

In the following, our intention is just to briefly mention the sets of isochrones which are the most useful for comparisons with observed photometric data, and to first mention some data that has not been published in precedence. A summary table of the available material is presented in Table 1.

5.1. An extended set of isochrones

Girardi et al. (2000) computed a set of low- and intermediate-mass stellar tracks which supersedes those previously used in Bertelli et al. (1994) isochrones. Additional models (unpublished) have been recently computed for initial chemical composition $[Z = 0.0001, Y = 0.23]$. Thus, we have created a new set of isochrones combining the latest low- and intermediate mass tracks (in the range $0.15 - 7.0\ M_\odot$) with the formerly available massive ones. The full references are given in Table 1.

In all cases in which "2000" and "1994" tracks have been combined, we find excellent agreement between the relevant quantities (lifetimes, tracks in the HR diagram) at the transition mass of $7-8\ M_\odot$. This is explained considering that the intermediate- and high-mass models share the same prescription for convection, and have interior opacities dominated by electron scattering (which has not been changed in the meanwhile). For the solar metallicity, we have combined tracks presenting slightly different initial metallicities – $[Z = 0.019, Y = 0.273]$ in Girardi et al. (2000), and $[Z = 0.020, Y = 0.280]$ in Bressan et al. (1993) – without finding any significant discontinuity.

Finally, to this extended set we have included the Marigo et al. (2001) isochrones for zero-metallicity stars.

5.2. Overshooting vs. classic models

For solar metallicity and in the mass range $0.15 - 7.0\ M_\odot$, Girardi et al. (2000) presents an additional set of tracks and isochrones computed with the classical semi-convective prescription for convective borders. Then, the two $[Z = 0.019, Y = 0.273]$ sets are useful if one chooses to compare classical with overshooting models. The same kind of work is being extended to metallicities $[Z = 0.004, Y = 0.240]$ and $[Z = 0.008, Y = 0.250]$ (Barmina et al. 2002), and will be included in the database when completed.

5.3. Solar-scaled vs. α-enhanced models

Salasnich et al. (2000) presents new models for 4 different metallicities ($[Y = 0.250, Z = 0.008]$, $[Y = 0.273, Z = 0.019]$, $[Y = 0.320, Z = 0.040]$ and $[Y = 0.390, Z = 0.070]$), computed both with scaled-solar and alpha-enhanced distributions of metals. The tracks cover the mass range from 0.15 to 20 $M_\odot$. They represent a valid alternative to the isochrones referred to in Sect. 5.1, but do not cover the low-metallicity interval. Anyway, it has been demonstrated by Salaris et al. (1993; see also Salaris & Weiss 1998; and VandenBerg 2000), that for low metallicities one may safely use scaled-solar stellar models instead of α-enhanced ones of same Z.

5.4. Simple vs. more detailed TP-AGB models

All the tracks and isochrone sets above mentioned, include the complete TP-AGB phase as computed with a simple synthetic algorithm (Girardi & Bertelli 1998). In parallel, Marigo (2001, and references therein) has developed a much more sophisticated code for synthetic TP-AGB evolution, which includes crucial processes such as the third

[5] Of course, they can also be applied to any other set of stellar data in the literature.

Table 1. Stellar tracks used in the different set of isochrones.

Initial chemical comp.:			Evolutionary tracks:					Isochrones:		
			Mass ranges (in $M_\odot$):[2]			TP-AGB	convec-	age range	filename in	basic
Z	Y	kind[1]	0.15–0.55	0.6–7.0	> 7.0	evolution[3]	tion[4]	$\log(t/\mathrm{yr})$	database	reference[2]
0.0	0.230	S	–	Ma01	Ma01	–	O	6.30 − 10.25	isoc_z0.dat	Ma01
0.0001	0.230	S	Gi01	Gi01	Gi96	G	O	6.60 − 10.25	isoc_z0001.dat	Gi01+Gi96
0.0004	0.230	S	Gi00	Gi00	Fa94a	G	O	6.60 − 10.25	isoc_z0004.dat	Gi00+Be94
0.001	0.230	S	Gi00	Gi00	–	G	O	7.80 − 10.25	isoc_z001.dat	Gi00
0.004	0.240	S	Gi00	Gi00	Fa94b	G	O	6.60 − 10.25	isoc_z004.dat	Gi00+Be94
0.008	0.250	S	Gi00	Gi00	Fa94b	G	O	6.60 − 10.25	isoc_z008.dat	Gi00+Be94
0.019	0.273	S	Gi00	Gi00	Br93	G	O	6.60 − 10.25	isoc_z019.dat	Gi00+Be94
0.030	0.300	S	Gi00	Gi00	–	G	O	7.80 − 10.25	isoc_z030.dat	Gi00
0.019	0.273	S	Gi00	Gi00	–	G	C	7.80 − 10.25	isoc_z019nov.dat	Gi00
0.008	0.250	S	Sa00	Sa00	Sa00	G	O	7.00 − 10.25	isoc_z008s.dat	Sa00
0.019	0.273	S	Sa00	Sa00	Sa00	G	O	7.00 − 10.25	isoc_z019s.dat	Sa00
0.040	0.320	S	Sa00	Sa00	Sa00	G	O	7.00 − 10.25	isoc_z040s.dat	Sa00
0.070	0.390	S	Sa00	Sa00	Sa00	G	O	7.00 − 10.25	isoc_z070s.dat	Sa00
0.008	0.250	A	Sa00	Sa00	Sa00	G	O	7.00 − 10.25	isoc_z008a.dat	Sa00
0.019	0.273	A	Sa00	Sa00	Sa00	G	O	7.00 − 10.25	isoc_z019a.dat	Sa00
0.040	0.320	A	Sa00	Sa00	Sa00	G	O	7.00 − 10.25	isoc_z040a.dat	Sa00
0.070	0.390	A	Sa00	Sa00	Sa00	G	O	7.00 − 10.25	isoc_z070a.dat	Sa00
0.004	0.240	S	Gi00	Gi00	–	M	O	7.80 − 10.25	isoc_z004m.dat	MG01
0.008	0.250	S	Gi00	Gi00	–	M	O	7.80 − 10.25	isoc_z008m.dat	MG01
0.019	0.273	S	Gi00	Gi00	–	M	O	7.80 − 10.25	isoc_z019m.dat	MG01

[1] S indicates a solar-scaled distribution of metals, A indicates an α-enhanced one. The adopted metal abundance ratios are specified in Salasnich et al. (2000).
[2] References for tracks and isochrones: Be94 = Bertelli et al. (1994, A&AS 106, 275); Br93 = Bressan et al. (1993, A&AS 100, 647); Fa94a = Fagotto et al. (1994a, A&AS 104, 365); Fa94b = Fagotto et al. (1994b, A&AS 105, 29); Gi96 = Girardi et al. (1996, A&AS 117, 113); Gi00 = Girardi et al. (2000, A&AS 141, 371); Gi01 = Girardi (2001, unpublished); Ma01 = Marigo et al. (2001, A&A 371, 152); MG01 = Marigo & Girardi (2001, A&A 377, 132); Sa00 = Salasnich et al. (2000, A&A 361, 1023).
[3] G means a simple synthetic evolution as in Girardi & Bertelli (1998), whereas M stands for more detailed calculations as in Marigo (2001; and references therein).
[4] O means a model with overshooting (see Gi00 for all references), whereas C corresponds to classical semi-convective models.

dredge-up and hot-bottom burning. Sets of complete TP-AGB tracks have been so far presented for metallicities $[Y = 0.240, Z = 0.004]$, $[Y = 0.250, Z = 0.008]$, and $[Y = 0.273, Z = 0.019]$ (Marigo 2001). A set of isochrones has been generated by combining these detailed TP-AGB tracks with the previous evolution from Girardi et al. (2000); they are presented in the appendix of Marigo & Girardi (2001).

These isochrones represent a useful alternative to the isochrones referred to in Sect. 5.1, any time the TP-AGB population is under scrutiny – for instance, when we have near-infrared photometry of objects above the RGB-tip. Marigo TP-AGB models are being extended to cover a larger metallicity interval.

6. Discussion and concluding remarks

6.1. Summary

This work is dedicated to the presentation of theoretical isochrones in several photometric systems. It represents the continuation of a wide project of the Padova group, started with Bertelli et al. (1994) and then carried on by Chiosi et al. (1997), and more recently by Salasnich et al. (2000). It starts describing the formalism for converting synthetic stellar spectra into tables of bolometric corrections (Sect. 2), in such a way that it can be easily applied to different photometric systems, and with the possibility of including extinction in a self-consistent way.

Then, we describe the assemblage of an updated library of stellar spectra (Sect. 3). The library is quite extended in $T_{\rm eff}$ and $\log g$, and includes the crucial dependence of spectral features on metallicity. Of course, it suffers from some limitations: very hot stars and M-giants are not included among synthetic spectra, a situation which can be remediated by using blackbody and empirical spectra, respectively. The strinkingly different spectra of carbon stars will also have to be considered in the future (Marigo et al., in preparation). These are probably the points where the models can be most improved. Moreover, several problems may be affecting the ATLAS9 synthetic spectra we are using to simulate the broad-band colours of most stars (see Sect. 3.1). Although such spectra have been demonstrated to be suitable for synthetic photometry (mainly for the Johnson-Cousins-Glass sys-

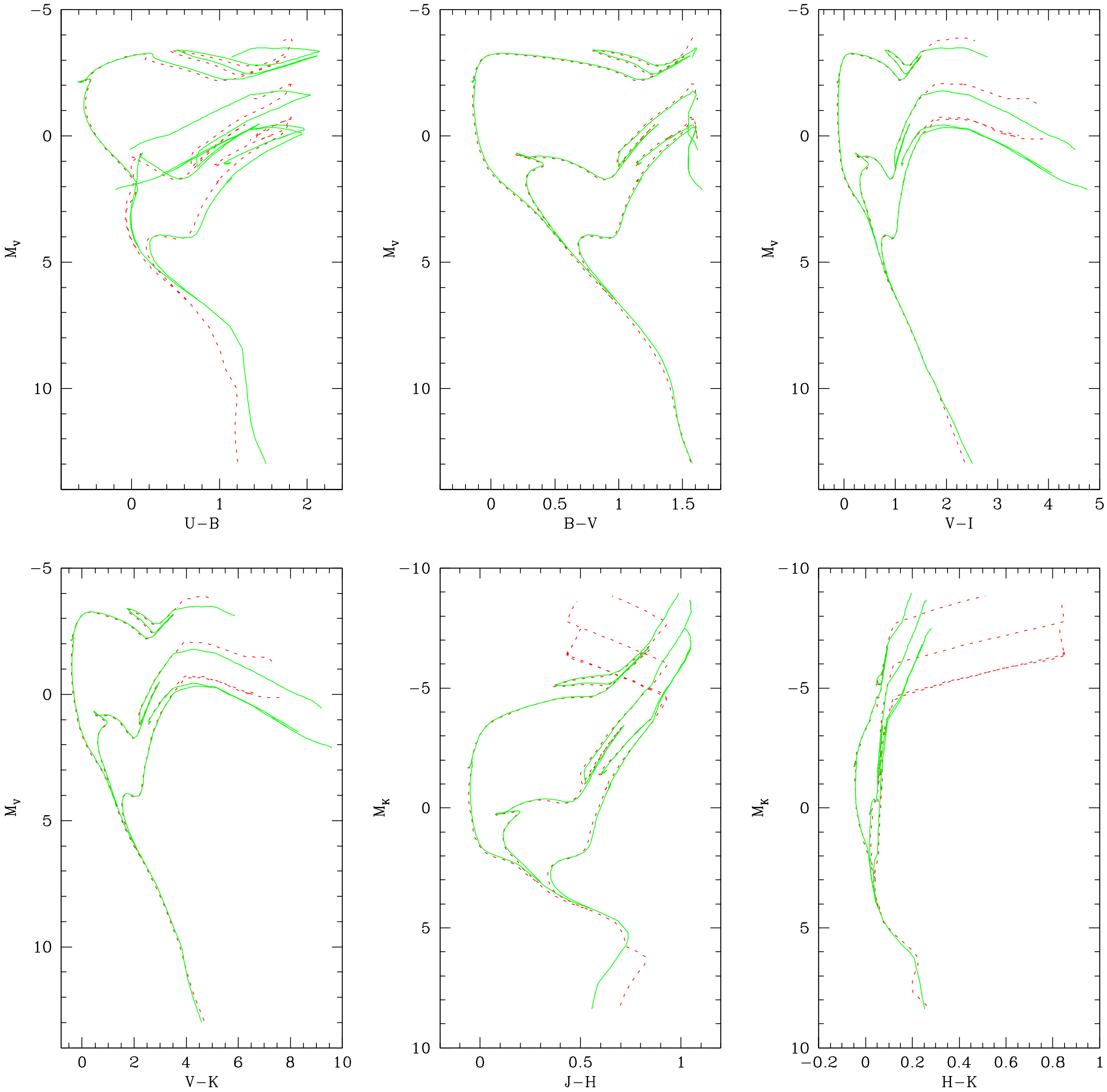

Fig. 4. Comparison of Girardi et al. (2000) isochrones transformed to Johnson-Cousins-Glass magnitudes and colours by using either present relations (continuous lines) or Bertelli et al. (1994) ones (dashed lines), in several CMDs. The isochrones have solar metallicity ($Z = 0.019$) and ages 10^8, 10^9, and 10^{10} yr (from top to bottom).

tem; e.g. Bessell et al. 1998), their accuracy has still to be sistematically evaluated for stars of all metallicities, temperatures and gravities. Anyway, we assume that they are good enough for simulating broad-band photometric systems in the visual-infrared wavelength region, whereas expect that the results in narrow-band systems, and in the ultraviolet pass-bands, will be affected by more significant errors. Another important aspect of synthetic spectra is that they are usually computed for scaled-solar chemical compositions, whereas the extension to peculiar and α-enhanced mixtures would be of high interest. This latter problem will probably be alleviated in a near future, with the release of extensions to ATLAS9 spectra.

From the spectral library, we derive bolometric corrections for each pass-band mentioned in Sect. 4, and apply them to the Padova isochrones. In practice, only in few cases we present newly-constructed isochrones: the bulk of isochrone data is already described in previous papers by our group, and it is only the transformation from theoretical quantities to absolute magnitudes that changes

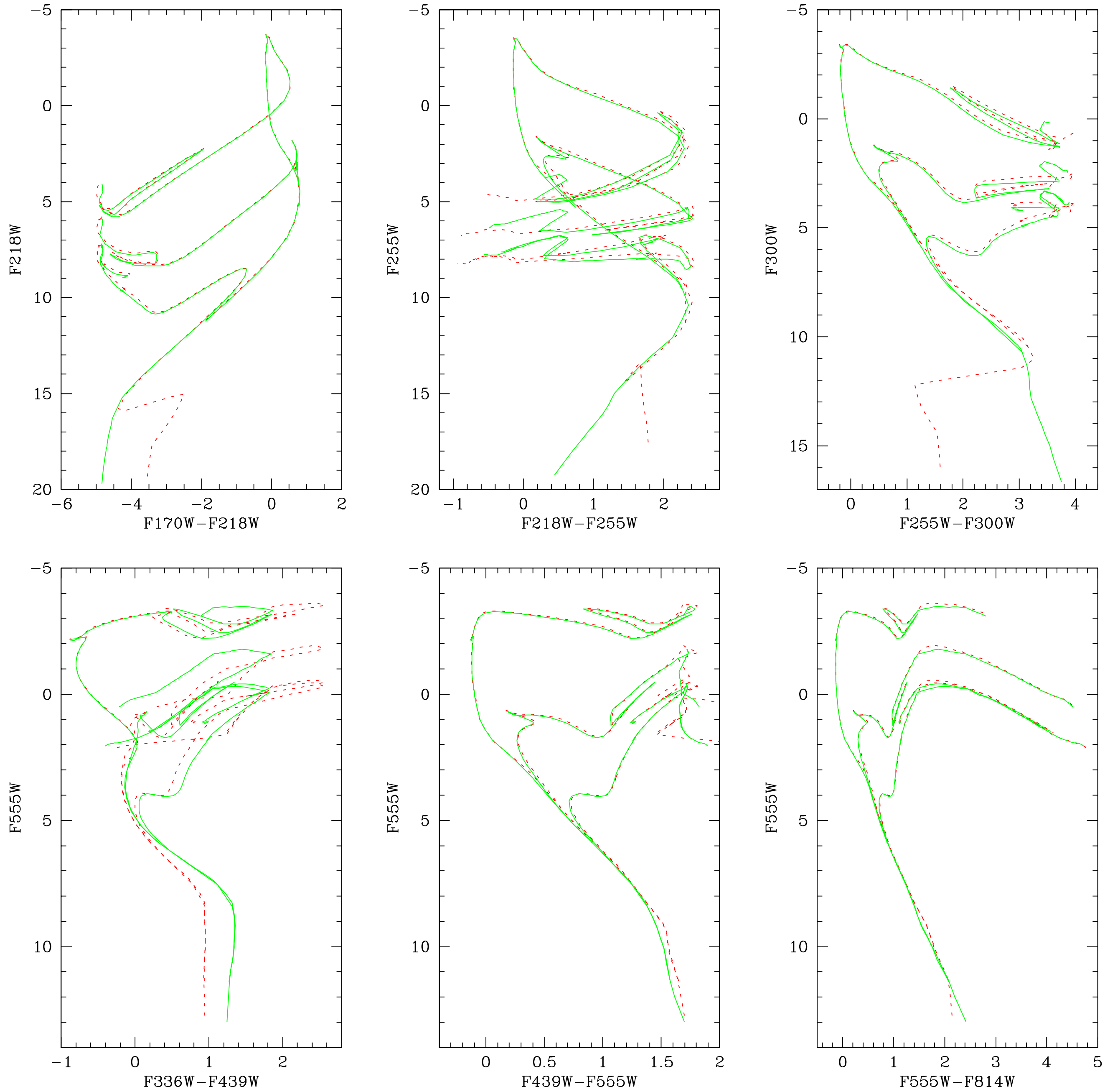

Fig. 5. Comparison of Girardi et al. (2000) isochrones as transformed to the WFPC2 VEGAmag system using either present relations (continuous lines) or Salasnich et al. (2000) ones (dashed lines). The isochrone ages and metallicities are the same as in Fig. 4.

compared to past releases. Sect. 5 summarizes the basic characteristics of the different sets of isochrones, indicating the full references.

6.2. Comparison with previous works

It is important to illustrate the differences between the present and previous transformations. The previous ones for $UBVRIJHK$ are fully described in Bertelli et al. (1994), and were adopted by Girardi et al. (2000), Salasnich et al. (2000) and Marigo et al. (2001); for HST/WFPC2 photometry, they are the ones described in Salasnich et al. (2000).

The situation for Johnson-Cousins-Glass is tentatively illustrated in Fig 4, which compares a set of Girardi et al. (2000) isochrones, transformed according to both present (continuous lines) and Bertelli et al. (1994; dashed lines) transformations. We point out that:

1. For stars hotter than $T_{\rm eff} \sim 4\,000$ K, present transformations are very similar to those of Bertelli et al.

(1994). The differences amount to just a few hundredths of a magnitude over most regions of the CMD, including the entire main sequence and subgiant branch, and most of the RGB. They can be entirely attributed to the slightly different pass-bands and zero-points, and to the use of more recent ATLAS9 "NOVER" atmospheres instead of Kurucz (1993) ones.
2. A somewhat similar situation holds for dwarfs cooler than $T_{\rm eff} \sim 4\,000$ K (see bottom end of the main sequence in all panels, for $M_V \gtrsim 7$, and $M_K \gtrsim 5$). The differences are generally small and can be attributed to the change from Kurucz (1993) to Allard et al. (2000a) spectra. The exceptions are $U-B$ and $J-H$ colours, for which the differences between the two versions become sizeable.
3. For giants cooler than 4 000 K, present transformations become very different. This can be noticed in the upper-right corner of all diagrams. M-giants corresponding to the RGB-tip and TP-AGB, are now seen to fade by some magnitudes in V, due to a sort of rapid increase of visual BCs at $T_{\rm eff} \lesssim 3\,500$ K. This effect is caused by the use of Fluks et al. (1994) spectra and their $T_{\rm eff}$ vs. $V-K$ scale. Such a bending of the RGB is indeed observed in CMDs of old metal-rich clusters (see e.g. Ortolani et al. 1990; and Rich et al. 1998), and seems to be better reproduced now than with previous transformations. Other differences appear in all colours: the most remarkable are the excursion of M-giants of latest type towards much bluer $U-B$, and the much smoother behaviour now obtained for $J-H$ and $H-K$.

A quite similar situation holds for HST/WFPC2 photometry, as illustrated in Fig. 5. This time, we compare the same isochrones as transformed with present (continuous lines) and Salasnich et al. (2000; dashed lines) transformations. It is evident that the present transformations ensure a more continuous behaviour of the colours for all low-temperature stars (both dwarfs and giants).

From the plots at the top row of Fig. 5, one can also appreciate the unusual appearance of isochrones in CMDs that involve ultraviolet WFPC2 pass-bands: Notice for instance that in F170W, F218W, F255W and F330W magnitudes, giants may be fainter than turn-off stars. Isochrones in the F218W vs. F170W−F218W and F255W vs. F218W−F255W diagrams are even "twisted", because the $T_{\rm eff}$ vs. colour relations are not monotonic for these filters. These effects are related to the presence of a red leak in the ultraviolet HST filters (for both the present WFPC2 and the former FOC camera), and are extensively discussed by Yi et al. (1995) and Chiosi et al. (1997).

As a consequence of the great similarity between present and previous $UBVRIJHK$ and HST/WFPC2 transformations, for most colours and over a large portion of the HR diagram, most results derived from previous Padova isochrones are not expected to change. Exceptions may show up for works that are concerned with the photometry of the reddest giants, with $T_{\rm eff} \lesssim 3\,500$ K ($B-V \gtrsim 1.5$), or that deal with low-mass main-sequence stars in the $U-B$ and ultraviolet colours.

6.3. New results

The greatest improvement of the present database is in the presentation of Padova isochrones in several photometric systems for which they were not available so far – including the case of brand-new systems. Three examples of theis kind are given in Figs. 6, 7 and 8.

First, Fig. 6 presents the isochrones in NICMOS ABmag system. In a VEGAmag system, NICMOS isochrones would look similar to their equivalent Johnson-Cousins-Glass ones, shown in Fig. 4. In the ABmag system, however, they appear shifted to quite different colour and magnitude intervals.

Figure. 7 illustrates how Padova isochrones look like in the T_1 vs. $C-T_1$ CMD of Washington photometry, both for varying age at constant metallicity (left panel), and for varying metallicity at constant age (right one). The striking feature in these plots is the excellent separation in metallicity offered by the $C-T_1$ colour, from the main sequence up to red giant phases. This feature, combined to the excellent throughput in the C filter (Fig. 3), is among the advantages that make the Washington system a very competitive one if compared to Johnson-Cousins (see also Paltoglou & Bell 1994, and Geisler & Sarajedini 1999).

Preliminary comparisons point to a good agreement between our Washington isochrones and real data for LMC fields from Bica et al. (1998). Just to mention an example, we notice that $C-T_1$ for giants "saturates" at ~ 3.4, both in the models and in the LMC data.

An example of "new" photometric system is provided by the WFI, which has broad-band filters very different from Johnson-Cousins ones. To illustrate the effect in colours, Fig. 8 shows exactly the same isochrones as seen in BVI CMDs using either Johnson-Cousins or WFI filters, and applying in both cases the VEGAmag definition of zero-points. The differences are striking. In particular, since the BV WFI filters represent a wavelength baseline shorter than the Johnson ones, they provide a more modest separation of stars in $B-V$ colour. It is evident from this plot that the normal Johnson-Cousins isochrones cannot be used to interpret WFI data that has been converted to VEGAmag or ABmag systems, as for most of EIS data (e.g. Arnouts et al. 2001; Groenewegen et al. 2002)[6].

6.4. Retrieval of electronic tables

All the data here mentioned are available at the WWW site `http://pleiadi.pd.astro.it`. The database already includes a very large number of files, and is expected to increase further as we publish data for other photometric systems. Thus, it is hard to describe here both the

[6] Notice, however, that part of the data released from EIS – namely the pre-FLAMES survey – is in fact converted into a standard Johnson-Cousins system (see Momany et al. 2001).

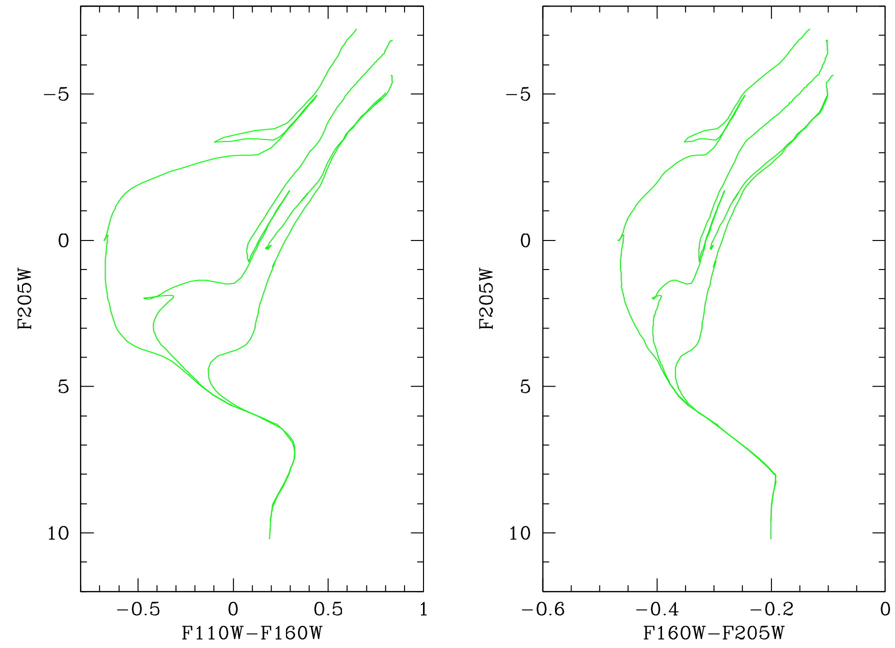

Fig. 6. Isochrones in the CMDs of NICMOS ABmag photometry. Ages and metallicities are the same as in Fig. 4.

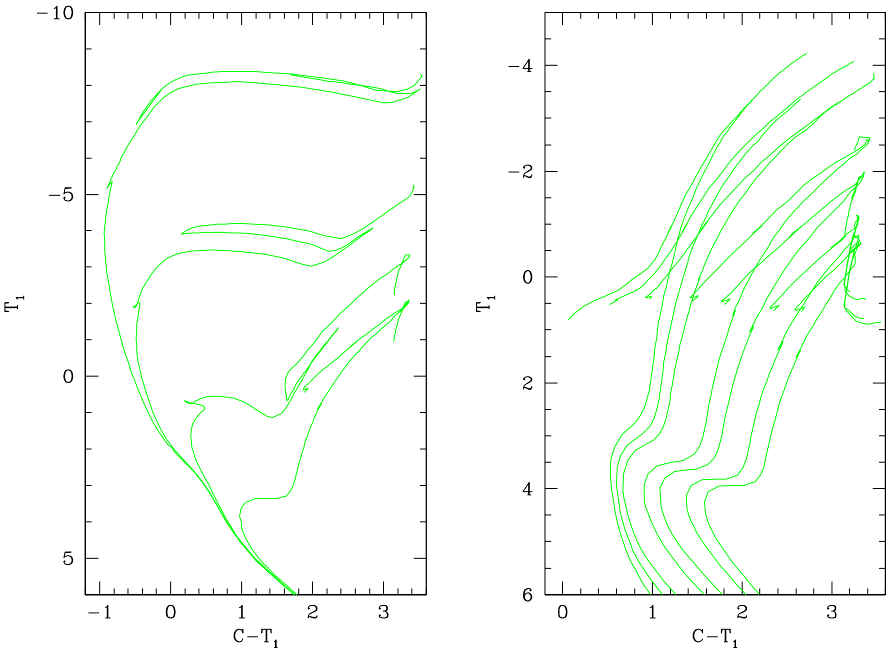

Fig. 7. Isochrones in the T_1 vs. $C-T_1$ plane of Washington photometry. Left panel: from top to bottom, a sequence of $Z = 0.008$ isochrones with ages 10^7, 10^8, 10^9, and 10^{10} yr. Right panel: from left to right, a sequence of 14 Gyr old isochrones with metallicities $Z =$ 0.0001, 0.0004, 0.001, 0.004, 0.008, 0.019, and 0.030.

structure of the database, and the content of each file. Moreover, this kind of information is probably useful just to whom actually accesses the database. Thus, we opt to provide all the relevant information in `readme.txt` files inserted in the database.

To the general reader, suffice it to briefly mention the kind of data which is available:

- Tables of bolometric corrections for each metallicity: they contain the quantities BC_{S_λ} for each filter, and as a function of stellar $T_{\rm eff}$ and $\log g$. Metallicities available are [Fe/H] = −2.0, −1.5, −1.0, −0.5, 0, +0.5. The values of $T_{\rm eff}$ and $\log g$ are not exactly the same for all metallicities, but correspond quite well to the regions indicated in Fig. 1.
- Tables of isochrones: they include all metallicities and cases indicated in Sect. 5. The various photometric systems are separated in different directories. For each isochrone file, the information and structure are the same as already presented in Girardi et al.

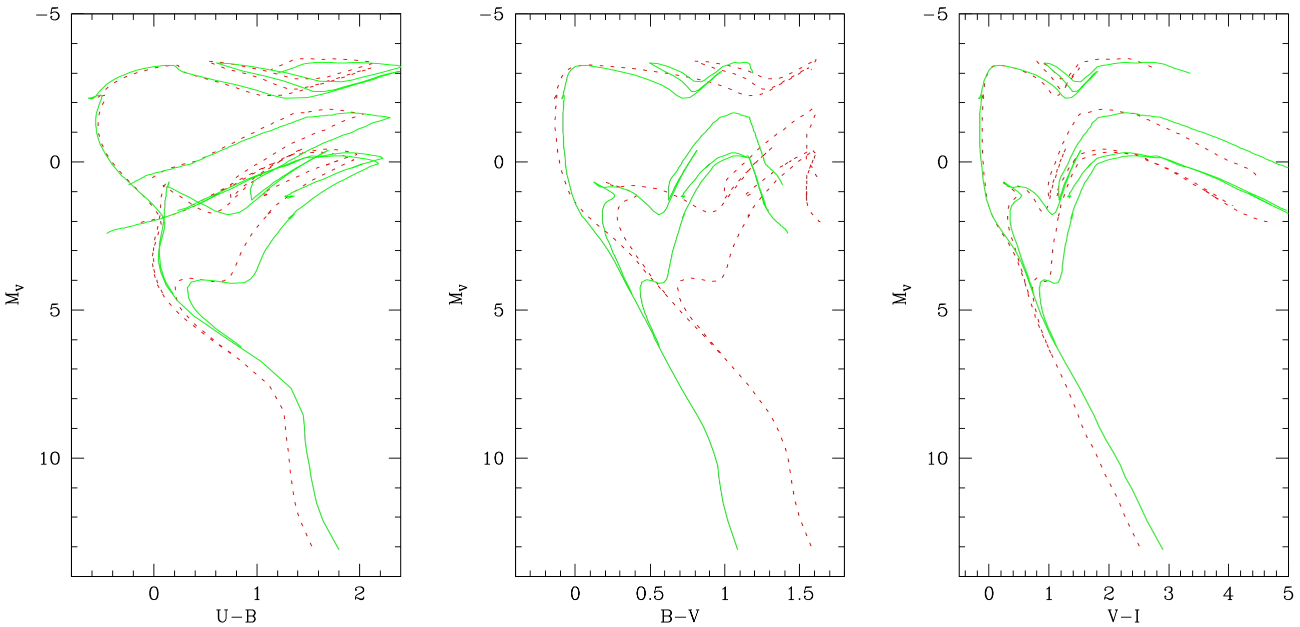

Fig. 8. Comparison between the same set of $Z = 0.019$ isochrones as seen in the $UBVI$ CMDs using either Johnson-Cousins (dashed lines) or WFI filters (continuous lines). VEGAmag systems are used in both cases. Ages are the same as in Fig. 4.

(2000), Salasnich et al. (2000), and Marigo & Girardi (2001), with the obvious difference that instead of $UBVRIJHK$ absolute magnitudes, in each file we tabulate the absolute magnitudes for the photometric system under consideration.
– Tables of integrated colours of single-burst stellar populations: a table of this kind is present for each isochrone table. They provide integrated magnitudes in each pass-band, as a function of age.

Acknowledgements. L.G. thanks the many people who helped by providing filter transmission curves and zero-points information (in particular E. Bica, D. Geisler, J. Holtzman, D. Figer, E. Grebel, M. Gregg, M. Rich, S. Arnouts, and L. da Costa). Particularly appreciated are the availability (R. Kurucz, F. Allard) and help with (I. Baraffe) on-line spectral data, the useful comments by B. Plez regarding cool giants, and the many useful remarks by R. Bell and M.S. Bessell, which greatly helped to improve this paper. Also acknowledged are those who kindly pointed out some mistakes in our preliminar releases of data. L.G. acknowledges a stay at MPA funded by the European TMR grant ERBFMRXCT 960086. This work was partially funded by the Italian MURST.

References

Allard F., Hauschildt P.H., Alexander D.R., & Starrfield S., 1997, ARA&A 35, 137
Allard F., Hauschildt P.H., Alexander D.R., Tamanai A., & Ferguson J.W., 2000a, in proceed. of "From giant planets to cool stars", ASP Conf. Series v. 212, (eds.) C.A. Griffith & M.S. Marley, p. 127
Allard F., Hauschildt P.H., & Schwenke D., 2000b, ApJ 540, 1005
Allard F., Hauschildt P.H., Alexander D.R., Tamanai A., & Schweitzer A., 2001, ApJ 556, 357
Allende Prieto C., Barklem P.S., Asplund M., & Ruiz Cobo B., 2001, ApJ 558, 830
Allende Prieto C., Asplund M., Garcia López R.J., & Lambert D.L., 2002, ApJ 567, 544
Alonso A., Arribas S., & Martínez-Roger C., 1998, A&AS 131, 209
Alonso A., Arribas S., & Martínez-Roger C., 1999a, A&AS 139, 335
Alonso A., Arribas S., & Martínez-Roger C., 1999b, A&AS 140, 261
Alvarez R., Lançon A., Plez B., & Wood P.R., 2000, A&A 353, 322
Alvarez R., & Plez B., 1998, A&A 330, 1109
Arnouts S., Vandame B., Benoist C., et al., 2001, A&A 379, 740
Asplund M., Ludwig H.-G., Nordlund A., & Stein R.F., 2000, A&A 359, 669
Baggett S., & Gonzaga S., 1998, ISR WFPC2 98-03
Bahcall J.N., Pinsonneault M.H., & Wasserburg G.J., 1995, Rev. Mod. Phys. 67, n.4, 781
Barklem P.S., Piskunov N., & O'Mara B., 2000a, A&A 355, 5
Barklem P.S., Piskunov N., & O'Mara B., 2000b, A&A 363, 1091
Barmina R., Girardi L., & Chiosi C., 2002, A&A 385, 847
Bell R.A., Paltoglou G., & Tripicco M.J., 1994, MNRAS 268, 771

Bell R.A., Balachandran S.C., & Bautista M., 2001, ApJ 546, L65
Bertelli G., Bressan A., Chiosi C., Fagotto F., & Nasi E., 1994, A&AS 106, 275
Bessell M.S., 1979, PASP 91, 589
Bessell M.S., 1990, PASP 102, 1181
Bessell M.S., 2001, PASP 113, 66
Bessell M.S., & Brett J.M., 1988, PASP 100, 1134
Bessell M.S., Castelli F., & Plez B., 1998, A&A 333, 231
Bica E., Geisler D., Dottori H., et al., 1998, AJ 116, 723
Bohlin R.C., Holm A.V., Harris A.W., & Gry C., 1990, ApJS 73, 413
Bressan A., Fagotto F., Bertelli G., & Chiosi C., 1993, A&AS 100, 647
Buser R., & Kurucz R., 1978, A&A 70, 555
Canterna R., 1976, AJ 81, 228
Castelli F., 1999, A&A 281, 817
Castelli F., & Kurucz R.L., 1994, A&A 281, 817
Castelli F., & Kurucz R.L., 2001, A&A 372, 260
Castelli F., Gratton R.G., & Kurucz R.L., 1997, A&A 318, 841
Chabrier G., Baraffe I., Allard F., & Hauschildt P.H., 2000, ApJ 542, 464
Chiosi C., Vallenari A., & Bressan A., 1997, A&AS 121, 301
Ciardi D.R., van Belle G.T., Thompson R.R., Akeson R.L., & Lada E.A., 2000, AAS 197, 4503
Code A.D., Bless R.C., Davis J., & Brown R.H., 1976, ApJ, 203, 417
Colina L., Bohlin R., & Castelli F., 1996, Instrument Science Report CAL/SCS-008
da Costa L., 2000, in From Extrasolar Planets to Cosmology: The VLT Opening Symposium, (eds.) J. Bergeron and A. Renzini, Springer-Verlag, Berlin, p. 192.
Edvardsson B., & Bell R.A., 1989, MNRAS 238, 1121
Fagotto F., Bressan A., Bertelli G., & Chiosi C., 1994a, A&AS 104, 365
Fagotto F., Bressan A., Bertelli G., & Chiosi C., 1994b, A&AS 105, 29
Flower P.J., 1997, ApJ 469, 355
Fluks M.A, Plez B., The P.S., et al., 1994, A&AS 105, 311
Fukugita M., Ichikawa T., Gunn J.E., et al., 1996, AJ 111, 1748
Geisler D., 1996, AJ 111, 480
Geisler D., & Sarajedini A., 1999, AJ 117, 308
Girardi L., & Bertelli G., 1998, MNRAS 300, 533
Girardi L., Bressan A., Chiosi C., Bertelli G., & Nasi E., 1996, A&AS 117, 113
Girardi L., Bressan A., Bertelli G., & Chiosi C., 2000, A&AS 141, 371
Grebel E.K., & Roberts W.J., 1995, A&AS 109, 293
Groenewegen M.A.T., Girardi L., Hatziminaoglou E., et al., 2002, A&A submitted.
Gunn J.E., & Stryker L.L., 1983, ApJS 52, 121
Hayes D.S., 1985, Calibration of fundamental stellar quantities, IAU Symposium 111, ed. D.S. Hayes, L.E. Pasinetti and A.G.D. Philip (Dordrecht, Reidel), p. 225
Hayes D.S., & Lathan D.W., 1975, ApJ 197, 593
Hauschildt P.H., Allard F., Ferguson J., Baron E., & Alexander D.R., 1999, ApJ 525, 871
Holtzman J.A., Burrows C.J., Casertano S., et al., 1995, PASP 107, 1065
Houdashelt M.L., Bell R.A., Sweigart A.V., & Wing R.F., 2000a, AJ 119, 1424
Houdashelt M.L., Bell R.A., & Sweigart A.V., 2000b, AJ 119, 1448
Kurucz R.L., 1993, in IAU Symp. 149: The Stellar Populations of Galaxies, eds. B. Barbuy, A. Renzini, Dordrecht, Kluwer, p. 225
Kurucz R.L., 1995, in Astrophysical Applications of Powerful New Databases. Joint Discussion No. 16 of the 22nd IAU General Assembly, ASP Conference Series, V. 78, (eds.) S.J. Adelman, and W.L. Wiese, publisher: Astronomical Society of the Pacific, San Francisco, California, p. 205
Landolt A.U., 1992, AJ 104, 340
Leggett S.K., Allard F., Dahn C., et al., 2000, ApJ 535, 965
Leggett S.K., Allard F., Geballe T.R., Hauschildt P.H., & Schweitzer A., 2001, ApJ 548, 908
Lejeune T., Cuisinier F., & Buser R., 1997, A&AS 125, 229
Lejeune T., Cuisinier F., & Buser R., 1998, A&AS 130, 65
Lupton R.H., Gunn J.E., & Szalay A.S., 1999, AJ 118, 1406
Marigo P., 2001, A&A 370, 194
Marigo P., & Girardi L., 2001, A&A 377, 132
Marigo P., Girardi L., Chiosi C., & Wood P.R., 2001, A&A 371, 152
Momany Y., Vandame B., Zaggia S., et al., 2001, A&A 379, 436
Neckel H., & Labs D., 1984, Sol. Phys, 90, 205
Oke J.B., 1964, ApJ 140, 689
Oke J.B., & Gunn J.E., 1983, ApJ 266, 713
Ortolani S., Barbuy B., & Bica E., 1990, 263, 362
Paltoglou G., & Bell R.A., 1994, MNRAS 268, 793
Plez B., 1999, in Asymptotic Giant Branch Stars, IAU Symp. 191, (eds.) T. Le Bertre, A. Lebre, and C. Waelkens, p. 75
Renzini A., & da Costa L., 1997, The Messenger 87, 23
Rich R.M., Ortolani S., Bica E., & Barbuy B., 1998, AJ 116, 1295
Ridgway S.T., Joyce R.R., White N.M., & Wing R.F., 1980, ApJ 235, 126
Salaris M., Chieffi A., & Straniero O., 1993, ApJ 414, 580
Salaris M., & Weiss A., 1998, A&A 335, 943
Salasnich B., Girardi L., Weiss A., & Chiosi C., 2000, A&A 361, 1023
Schmidt-Kaler T., 1982, in: Landolt-Börnstein, Neue Serie VI/2b. Springer-Verlag, Berlin, 453-455, pp. 15-18

Straizys V., & Zdanavicius K., 1965, Bull. Vilnius Obs. 14, 1
Thuan T.X., & Gunn J.E., 1976, PASP 88, 543
Tsuji T., Ohnaka K., & Aoki W., 1996, A&A 305, 1
Tsuji T., Ohnaka K., & Aoki W., 1999, ApJ 520, 119
VandenBerg D.A., 2000, ApJS 129, 315
Yi S., Demarque P., & Oemler Jr. A., 1995, PASP 107, 273
Worthey G., 1994, ApJS 95, 107